9th AUSTRALASIAN
FLUID MECHANICS CONFERENCE,
AUCKLAND, 8-12 DECEMBER 1986

A Study of the Undular Jump Profile

J. S. MONTES

Department of Civil & Mechanical Engineering, University of Tasmania, Hobart, Tasmania, Australia.

1 INTRODUCTION

The subject of the normal or direct hydraulic jump has been extensively studied in most types of open channels, but comparatively little has been written on the allied phenomenon, the so called "undular jump".

The undular jump is the transition water surface profile from a weakly supercritical flow to a weakly supercritical flow. Throughout the length of this transition, the water surface has a wave like profile of diminishing amplitude which may extend for a considerable distance downstream. The surface is almost free of the rough and turbulent appearance associated with the normal jump, with the exception of the first crest, in which such turbulence occasionally appears (Fig. 1).

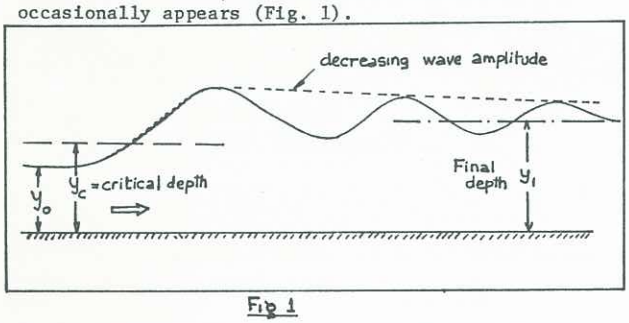

Fig 1

It has been experimentally determined (Bakhmeteff 1936) that the value of the initial Froude No. which separates the normal from the undular jumps in rectangular channels is about 1.73, which corresponds to a ratio of the conjugate depths y_1/y_0 of about 2. For larger Froude numbers, the jump takes the conventional form of a rather short, steep and highly turbulent standing wave front.

Because the limit Fr = 1.73 is easily exceeded in flow in steep channels or immediately below sluice gates, the generation of stable undular jumps is no trivial matter, even under controlled laboratory conditions. They are seldom seen in nature. Due to the experimental difficulty of generation, the study of the jumps has often been made through the observation of the translatory wave called the "undular bore". Such waves can be generated by sudden variations of the discharge of a weakly supercritical flow, and can be theoretically reduced to the undular jump by a single kinematic transformation. Undular bores are common in hydropower canals after load rejection maneuvers, or in estuaries where the tidal range is considerable. The analysis of the bore is generally confined to the case of the wave advancing on still water of constant depth (Favre (1935), Keulegan and Patterson (1940), Sandover and Zienkewicz (1957)), etc.).

The kinematic transformation to a stationary wave is possible due to the fact that the wave moves at nearly constant velocity, so that the momentum and energy equations for steady flows may be now employed in a frame of reference attached to the first modulation of the wave train. Although this formalism is plausible, such transformation does not recognize the considerable difference in boundary layer formation under the bore and under the undular jump. Under a bore the boundary layer develops in a favorable pressure gradient (pressure decreasing in the direction of motion), and thus remains thin and attached to the bottom of the channel. In the undular jump, the boundary layer existing on the supercritical flow encounters a sharply rising pressure gradient. It is found then that it thickens rapidly and is liable to separation from the bottom, a circumstance which can be verified in the laboratory and has been reported previously by Einwachter (1935).

Fig. 2 sketches this fundamental difference.

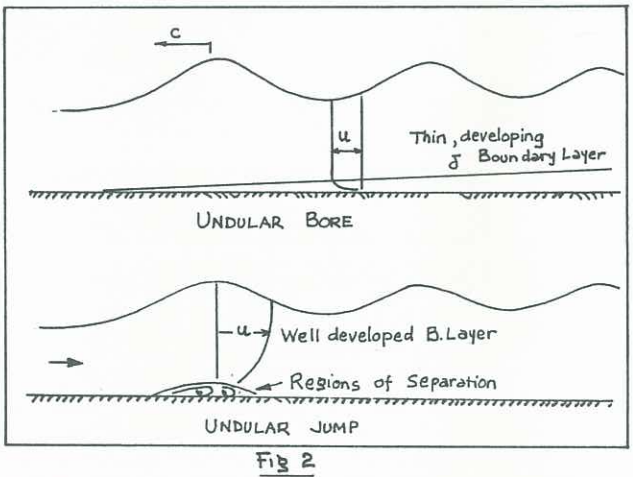

Fig 2

The difference in boundary layer development in the bore and in the jump has an obvious influence on the stability of the water surface. In the jump, the region above the separation bubble, located almost always below the first crest has a rough appearance and may break into a roller similar to that found in the normal jump. The bore, in contrast, shows a smooth, unruffled surface to values of Froude number well in excess of those indicating wave breaking in the undular jump.

The passage of flow through critical depth is accompanied by the appearance of transversal (Mach) waves on the surface. Such waves can also be observed over the standing wave formed over long broad crested weirs, although they are less marked than those over the undular jump. The reason for the Mach waves is not clear, but it is suggested that they may be connected with the existence of a lateral boundary layer, which, by retarding the fluid near the wall forces a transition through critical depth sooner than for the fluid near the centre. The effective width of the channel is thus progressively reduced downstream, and the Mach waves seen in experiment are identical to those obtained by small deflections of the lateral boundaries (Fig. 3).

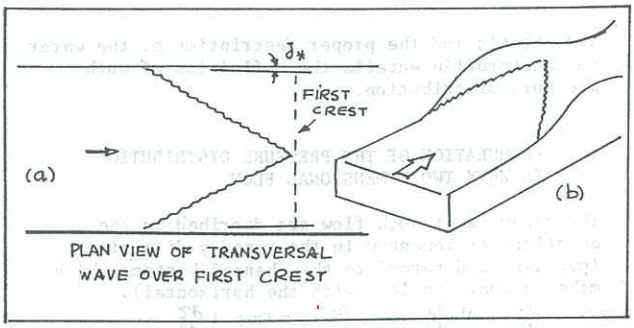

Fig. 3

When the transversal waves meet at the centre of the flow they generate a higher wavelet or "cox-comb" which may be significantly higher than the rest of the surface (Fig. 3-b). The existence of the surface transversal waves and of a region of separation beneath the first crest are features which suggest a certain three dimensionality of the flow in this region of the undular jump. By contrast, the flow near the leading wave of the undular bore is free from Mach waves and exhibits in general a glossy, smooth surface. This characteristic is far from having only a purely "cosmetic" importance. The existence of the undular jump depends to a marked degree on the available energy and very small departures from the values of E found in the parallel supercritical flow preceding the jump will force a transition to an ordinary type of jump, as explained in Fig. 2. It also follows that the calculation of energy losses in the jump is extremely difficult, not only because of the wavy surface, and adverse pressure gradients on the bottom boundary layer, but also because of the two local sources of energy dissipation pointed above. In the case of the undular bore, relatively simple boundary layer calculations have enabled Hawaleshka and Savage (1966) and other authors to obtain good agreement between measured and computed water surface profiles.

2 EXISTENCE OF THE UNDULAR JUMP, EXPERIMENTAL STUDIES

Early experimenters, such as Darcy and Bazin (1865) observed and described the undular jump. In their case, the jump was produced in a channel of moderate slope, in which the Froude number of the flow was below Fr = 2. Favre (1935) found experimentally that undular jumps appear when the ratio of initial to critical depth, y_o/y_c , exceeds 0.67, equivalent to a Froude number of 1.57. Only conventional jumps (with rollers on the free surface) can exist for

$$y_o/y_c < 0.61 \qquad (F_o > 1.71)$$

Bakhmeteff (1936), in a study of conventional hydraulic jumps which is one of the most important contributions to this subject, proposed a criterion for the formation of undular jumps:

$$F_o < \sqrt{3}$$
$$y_1/y_o < 2$$

which rests upon the following argument: the ratio between initial and sequent depth for a conventional jump is:

$$\frac{y_1}{y_o} = \frac{1}{2}\left(\sqrt{1+8F_o^2} - 1\right) \qquad (1)$$

while the initial energy of the flow is:

$$E = y_o(1 + F_o^2/2)$$

Thus the ration of sequent depth to initial energy:

$$\frac{y_1}{E} = \frac{\sqrt{1+8F_o^2} - 1}{2 + F_o^2} \qquad (2)$$

This relation has a maximum for $F_o = \sqrt{3}$, indicating that such jump is the highest for its initial energy. It is likely that this explanation was prompted by the fact that the leading wave of the undular jump is higher than that indicated by (1).

Experiments by Ovalle and Dominguez (1934) revealed that only undular jumps were possible if y_o/y_c exceeded 0.733 (Fr = 1.593), but that, if special precautions were taken, undular jumps could persist up to ratios

$$\frac{y_o}{y_c} = 0.423 \qquad (F_o = 3.63)$$

The reasons for the passage of water surface profile from an undular form with low energy dissipation to one where the extent of the flow expansion is short and turbulent is explained in Sec. 3.

3 THE LIGHTHILL-BENJAMIN DIAGRAM

A convenient way of explaining the existence of undular jumps has been suggested by Benjamin & Lighthill (1954). Briefly, in open channel, steady flow there are two convenient parameters which describe the flow regime: the specific energy $E = y + q^2/2gy^2$ (y=total depth, q=unit discharge), and the specific momentum $M = q^2/gy + y^2/2$
Presented in dimensionless form, they are:

$$E_* = \frac{E}{y_c} = \eta + \frac{1}{2\eta^2} \qquad (3)$$

$$M_* = \frac{M}{y_c^2} = \frac{1}{\eta} + \frac{\eta^2}{2} \qquad \left(\eta = \frac{y}{y_c}\right) \qquad (4)$$

This pair of equations may be viewed as the parametric representation of the relation between M and E , and as such is plotted in Fig. 4. The function $M_* = f(E_*)$ is seen to have two branches intersecting at the point 1.5, 1.5 which is of course the minimum value which either function could have in parallel, steady flow. There are two branches: subcritical and supercritical. The domain of variation of the specific momentum and energy is divided into 3 distinct regions by the two branches. The boundaries, the lines themselves represent the only possible relation for M_* vs E_* when the flow is parallel and steady. The undular jumps are contained in the region between the two branches. The regions outside are not accessible to steady flows. Line AB in figure 4 represents the variation of energy in a flow which starts from the supercritical branch and ends on a parallel flow with same momentum on the subcritical branch, in other words, this represents the energy loss for the direct hydraulic jumps. The inscribed values of the relative depth on both branches furnish the conjugate depths of the jump. The mechanism of energy reduction is quite complex but one may suggest four possible contributions.

1. By shear at bottom and sides of the channel.
2. By turbulent energy dissipation at the surface, after the break of the first wave.
3. By maintenance of regions of recirculating fluid, a roller at the surface of energetic jumps (Fr 3) and smaller rollers at the separation regions at the bottom.
4. By energy radiated forward into the train of stationary waves.

The decrease in momentum due to these processes will come mainly from shear forces at the wetted perimeter. Let us assume that it is represented by the difference BB' on Fig. 4. If the energy decrease is less than AB , the M_*, E_* relation cannot satisfy the parallel flow condition and the jump remains undular. On the other hand if the loss is greater than AB' the flow is again incompatible with steady state conditions and the jump will not be stationary.

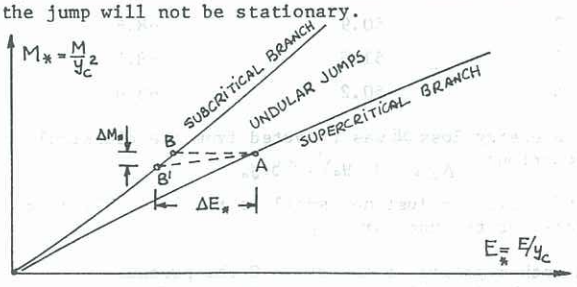

Fig. 4 The Benjamin-Lighthill diagram.

4 ENERGY BALANCE IN AN UNDULAR JUMP; THE PRESSURE DISTRIBUTION

Consider now the specific energy diagram E = f(y). The two points 0 and 1 represent the initial and final conditions of parallel flow for which

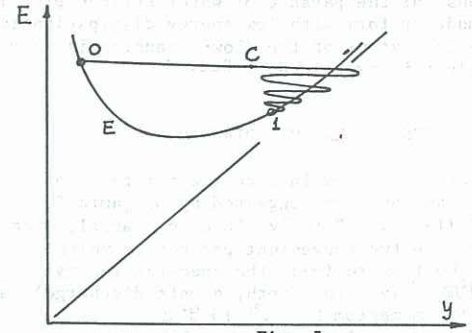

Fig. 5

$$E = y + \frac{q^2}{2gy^2}$$

Between 0 and 1 the E = E(y) relation will be that shown by the wavy line C which asymptotes to the parallel flow E curve. This relation is not possible unless the basic assumption on which the specific energy curve E was constructed, namely, the hydrostatic pressure distribution of the flow, is now relaxed.

A more general definition of the specific energy is:

$$E = \frac{1}{y}\int_0^y \left(z + \frac{p}{\rho g} + \frac{V^2}{2g}\right) dz \qquad (5)$$

If the pressure is considered to be composed of a hydrostatical component $\rho g(y-z)$ and a dynamical component p_d, the energy equation is:

$$E = y + \beta\frac{q^2}{2gy^2} + \frac{1}{y}\int_0^y \left(\frac{p}{\rho g} + \frac{v^2}{2g}\right) dz \qquad (6)$$

The last two terms are due to the effect of flow curvature and will be shown in Sec. 5 to amount to:

$$\frac{q^2}{3gy^2}\left(yy'' - \frac{y'^2}{2}\right) \quad , \text{ thus:}$$

$$E = y + \beta\frac{q^2}{2gy^2} + \frac{q^2}{3gy^2}\left(yy'' - \frac{y'^2}{2}\right) \qquad (7)$$

as in general the slope of the water surface is small, it follows that the intersections between the curves C and E in Fig. 5 will be at the points where $y'' \simeq 0$, near the points of inflection of the water surface profile.

An experimental proof for this assertion was obtained in a series of runs conducted at the Laboratory of Hydraulics of the University of Tasmania. For example, in run No. 9 the inflection points of the first four waves of the undular jump are indicated in Table No. 1.

Run No. 9
Initial depth y_0 = 37.0mm
Conjugate depth y_1 = 53.1mm
Froude No. F_1 = 1.323
Max. Energy Loss ΔE = 0.53mm.
$\frac{y_0}{y_c}$ = 0.829

Wave	$y_{inflection}$ (mm)	E at y_i (mm)
1	51.5	68.8
2	50.9	68.6
3	51.3	68.7
4	50.2	68.4

The energy loss ΔE was computed from the classical equation: $\Delta E = (y_1 - y_0)^3 / 4 y_1 y_0$

and indicates just how small is the allowable head loss for the undular jump.

At other points of the curve C the pressure distribution will be quite different from the hydrostatic and the proper description of the water surface profile entails the definition of such pressure distribution.

5 FORMULATION OF THE PRESSURE DISTRIBUTION IN WAVY TWO DIMENSIONAL FLOW

The dynamics of such flow are decribed by the equations of momentum in the x and y direction (parallel and normal to the channel bottom, which makes a small angle with the horizontal).

$$u\frac{\partial u}{\partial x} + v\frac{\partial u}{\partial z} = -\frac{1}{\rho}\frac{\partial p}{\partial x} + g\sin\theta + \frac{\partial \tau}{\partial z} \qquad (9)$$

$$u\frac{\partial v}{\partial x} + v\frac{\partial v}{\partial z} = -\frac{1}{\rho}\frac{\partial p}{\partial z} - g\cos\theta + \frac{\partial \tau}{\partial x} \qquad (10)$$

together with the continuity equation:

$$\frac{\partial u}{\partial x} + \frac{\partial v}{\partial z} = 0 \qquad (11)$$

The surface and bottom boundary conditions are:

at the surface z = y $\quad v = u_s\frac{\partial y}{\partial x}$ (12)
$\quad p = 0$

and at bottom z = 0 $\quad v = 0$ (13)

The left hand side of equations (9) and (10) may be reduced with the help of the continuity equation to the expressions:

$$u\frac{\partial u}{\partial x} + v\frac{\partial u}{\partial z} = -u^2\frac{\partial}{\partial z}\left(\frac{v}{u}\right) \qquad (14)$$

$$u\frac{\partial v}{\partial x} + v\frac{\partial v}{\partial z} = u^2\frac{\partial}{\partial x}\left(\frac{v}{u}\right) \qquad (15)$$

The ratio between the transversal and logitudinal velocities is now related to the boundary conditions of the problem. At the surface: $\frac{v}{u} = \frac{\partial y}{\partial x}$

and at bottom $\frac{v}{u} = 0$

One may assume with Boussinesq (1868) that at intermediate points the ratio $\frac{v}{u}$ is given by the linear relation:

$$\frac{v}{u} = \frac{z}{y}\frac{\partial y}{\partial x} \qquad (16)$$

Serre (1953) is led to the same expression through a different argument. By inserting this relation into the momentum equations one finds:

$$-\frac{u^2}{y}\frac{\partial y}{\partial x} = -\frac{1}{\rho}\frac{\partial p}{\partial x} + g\sin\theta + \frac{\partial \tau}{\partial z} \qquad (17)$$

$$\frac{z}{y}\frac{u^2}{y}(yy'' - y'^2) = -\frac{1}{\rho}\frac{\partial p}{\partial z} - g\cos\theta + \frac{\partial \tau}{\partial x} \qquad (18)$$

The variation of pressure in the vertical direction is obtained by integrating this last equation, using the boundary condition p = 0 at z = y and neglecting the small term $\partial\tau/\partial x$

$$p(z) = \rho g\cos\theta(y-z) + \frac{(yy'' - y'^2)}{y^2}\int_z^y u^2 z\, dz \qquad (19)$$

The integral term on the right hand side of this equation may be evaluated by postulating that amywhere in the channel the velocity distribution is given by:

$$u = \alpha U\left(\frac{z}{y}\right)^{1/N} \qquad (20)$$

where U is the mean velocity: q/y and N a constant. This type of self-similar distribution has been widely employed in boundary layer analysis. The constant N is taken as approximately 7 to 10 depending on the Reynolds number of the flow. Under this assumption the pressure distribution is then:

$$p(z) = \rho g(y-z) + \rho U^2\left(\frac{N+1}{N}\right)(yy'' - y'^2)\left(1 + \left(\frac{z}{y}\right)^{(2N+1)/N}\right) \qquad (21)$$

in the case of uniform velocity distribution ($N \to \infty$) we retrieve Serre's equation:

$$p(z) = \rho g(y-z) + \frac{1}{2}\rho U^2(yy' - y'^2)\left(1 - \left(\frac{z}{y}\right)^2\right) \qquad (22)$$

The dynamic contribution to the pressure distribution is seen to depend on the curvature of the water surface. For the crests of the waves $y'' < 0$ and the total pressure is less than the hydrostatical, the situation is reversed at the troughs.

Given the vertical velocity distribution, equation (16), horizontal velocity distribution (20) and pressure distribution (21), one finds for the generalized specific energy (equation 9):

$$E = y\cos\theta + \frac{(N+1)^2}{N(2N+2)}\frac{U^2}{2g} + \frac{(N+1)^2}{N(3N+2)}\frac{U^2}{g}(yy'' - \frac{y'^2}{2}) \qquad (23)$$

The coefficient of the term $\frac{U^2}{2g}$ is seen to be the Boussinesq velocity distribution parameter β. Again, by assuming uniform velocity distribution, (23) reduces to the expression (9) quoted in Sec. 4.

6 WATER SURFACE PROFILE OF THE UNDULAR JUMP

As the local depth y of the undular jump satisfies the differential equation (23), one may obtain the surface profile by integration of this equation, on the assumption that the local value of E could be formulated in terms of x and y.

Given the arguments considered in Sec. 3, it seems that the energy dissipation in the jump is a very complex phenomenon, and thus the steady state approximation:

$$\frac{dE}{dx} = S_o - \frac{U^2}{C^2R} \qquad (24)$$

where C = Chezy coefficient and R = hydraulic radius can but roughly describe the true situation. In spite of this caveat such integration will now be attempted. To simplify the problem, it is convenient to scale the depths and horizontal distances in terms of the critical depth y_c. Thus, with $\eta = y/y_c$ and $\zeta = \frac{x}{y_c}$ we find:

$$E_* = \eta + \frac{\beta}{2\eta^2} + \frac{m}{\eta^2}(\eta\eta'' - \eta'^2) \qquad (25)$$

$$\frac{dE_*}{d\zeta} = S_o - \frac{f}{8}(1+2\frac{y_c}{b}\eta)/\eta^3 \qquad (26)$$

valid for a rectangular channel with width b and small slope.

A first integral of (25) may be obtained by recognizing that:

$$\frac{1}{\eta^2}(\eta\eta'' - \eta'^2) = \frac{1}{2}\frac{d}{d\eta}(\frac{\eta'^2}{\eta}) \qquad (27)$$

so that: $$\frac{\eta'^2}{\eta} = \frac{\eta_o'^2}{\eta_o} + \frac{2}{m}\int_{\eta_o}^{\eta}(E_* - \eta - \frac{\beta}{2\eta^2})\,d\eta \qquad (28)$$

If the initial conditions are that the undular jump starts from parallel flow, then Hence

$$\eta'^2 = \frac{2\eta}{m}\left(\int_{\eta_o}^{\eta} E_*\,d\eta - \frac{1}{2}(\eta^2 - \eta_o^2) + \frac{\beta}{2}(\frac{1}{\eta} - \frac{1}{\eta_o})\right) \qquad (29)$$

Although (29) affords a powerful and simple condition for the existence of a solution of the system (25) and (26), this can only be obtained by numerical integration.

7 NUMERICAL INTEGRATION OF THE SYSTEM

It was found that the integration of the system was not easy. Several standard integration methods, such as Milne's 4th order predictor corrector proved unstable. After considerable testing, the 4th order single-step method of Bulirsch-Stoer (Acton, 1970) proved most suitable. All methods were extremely sensitive to the correct evaluation of the specific energy term E. This is not surprising in the light of the previous discussion: the energy loss within the jump must be confined between narrow limits for the undular jump to be possible. This condition is also implicit in equation (29), in which the value of E must be defined so as to allow η'^2 to remain always positive. For this reason, the slope and frictional terms in the numerical calculation must be specified very precisely. Given the approximation involved in the computation of energy losses, it is not entirely unexpected that the comparison between computed and measured profiles is not satisfactory. The first crest was not too badly reproduced, but the damping of the amplitude of the calculated profile is much less than the experimental values. Further progress in the areas of numerical computation and estimation of energy is evidently necessary.

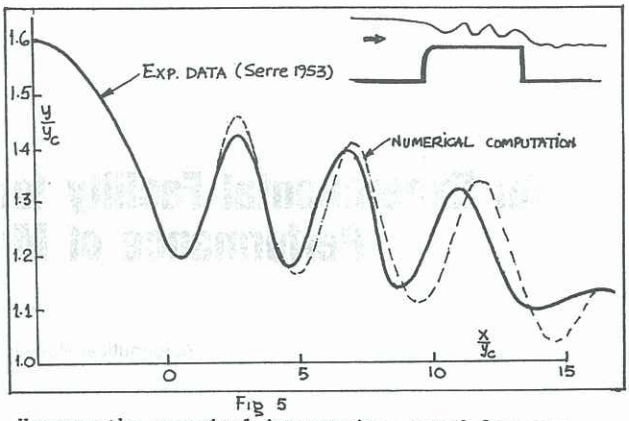

Fig 5

However the numerical integration proved far more successful in the solution of a similar problem. Fig. 6 shows the comparison of the undular profile created over a very rough and long broad crested weir (experimental data from Serre 1953). Both the wave shape and length are well predicted by numerical method, except at the end where the flow went into a free overfall. It must be remarked that the undular flow is entirely confined within the subcritical regime, thus no localized losses due to wave breaking or Mach waves was apparent.

REFERENCES

Acton, F. Numerical Methods that work. Harper & Row, 1970.

Bakhmeteff, B. and Matzke, A. "The Hydraulic Jump in terms of Dynamic Similarity". Transactions, American Society of Civil Engineers, 1936.

Benjamin, T.B. and Lighthill, J. "On cnoidal waves and bores". Proceedings, Royal Society of London, A, 224, pp.448-460, 1954.

Boussinesq, J. "Essai sur la theorie des eaux courantes". Memoires, Academie des Sciences, Paris, 23, 1877.

Darcy, H. and Bazin, H. "Recherches Hydrauliques, 1ère Partie: recherches experimentales sur l'ecoulement de l'eau dans les canaux decouverts". Academie de Sciences, Paris, 1865.

Einwachter, J. "Wassersprung und Deckwalzen lange". Wasserkraft und Wasserwirtschaft, 30, 8, 85-88, 1935.

Favre, H. Ondes de translation dans les canaux decouvertes. Dunod, Paris, 1935.

Hawaleska, O. and Savage, S.B. "The Development of Bores with Friction". Coastal Engineering Conference Proceedings, 1966, pp.461-472.

Keulegan, G. and Patterson, G.W. "Mathematical Theory of Irrotational waves". Bureau of Standards, Washington, D.C., U.S.A., Jan. 1940.

Ovalle, A. and Dominguez, A., Civil Engineering Thesis, Catholic University, Santiago, Chile, 1934.

Sandover, J.A. and Zienkewicz, O. "Experiments on Surge Waves". Water Power, November 1957, pp.418-424.

Serre, F. "Contributions a l'etude des ecoulements permanents et variables dans les canaux". La Houille Blanche, 3, pp.374-388, June-July and 6, pp.830-872, December 1953.